数理解析研究所講究録
1152巻 2000年 91-105

Spiral Structures in Magnetized Rotating Plasmas

Mitsuo Kono

Faculty of Policy Studies, Chuo University, Hachioji, Tokyo 192-0393, Japan,

Masayoshi Y. Tanaka

National Institute for Fusion Sciences, Toki, Gifu 509-5292, Japan

Abstract

A theory of spiral structure formation has been formulated to show that spiral structures are rather basic entities in magnetized rotating plasmas subjected to various kind of instabilities such as collisional drift wave instability, flute mode instability due to centrifugal force, and Kelvin-Helmhotz instability. The characteristic features of spiral structures observed experimentally in ECR plasmas are reproduced by our theory.

52.30q, 52.35kt, 52.35Py

Self-organized structures in magnetized plasmas have been a topic since they may give a deep insight into self-organization in complex systems as well as transport phenomena in plasmas. Coherent structures have been recently observed in laboratories [1–6] and are subjects of theoretical analysis for understanding underlying physics [7]. In both ECR plasmas [4] and gun-produced plasmas [5], two-arms spirals are commonly observed, and in particular the spiral structure observed in the ECR plasmas have interesting features: (1) the stationary structure is observed in a certain range of the background pressure, (2) the direction of the arm stretching is reversed when the magnetic field is reversed, and (3) the arm winding is identified as an Archimedes spiral, that is the curve spiraling into the origin which in polar coordinates is given by the equation $r \propto \theta$.

In the ECR plasmas, the ratio of the ion-neutral collision frequency to the ion cyclotron frequency is small as $\nu_i/\Omega_i \sim 0.05$, and the azimuthal rotation due to $\mathbf{E} \times \mathbf{B}$ drift, which is $0.2 \sim 0.4C_s$ (C_s: ion acoustic velocity), dominates the radial drift due to collisions. Furthermore, the ratio of the nonlinear term to the Lorenz force term $C_s/r_d\Omega_i$ is as small as ν_i/Ω_i, where r_d is the plasma radius. Thus, we can deal with the problem of spiral formation using the linear approximations.

In this letter, we show that low frequency perturbations ($\omega \ll \Omega_e$, Ω_e: electron cyclotron frequency) in an azimuthally rotating plasma may develop into spiral structures, which, in a particular case, are stationary. Instabilities such as the collisional drift wave instability, centrifugal instability and Kelvin-Helmholz instability are taken into account, and the linear eigen-value problem for the perturbed potential is numerically solved to show the existence of spiral solutions.

The spiral structures in the gun-produced plasmas [5], in which ν_i is comparable with Ω_i, and the ion azimuthal flow is supersonic, will be discussed separately since full nonlinear treatment is required because of no smallness parameters.

Plasmas in a cylindrical vessel are inevitably driven to rotate with the $\mathbf{E} \times \mathbf{B}$ drift due to the ambipolar potential. Then the ions are subjected to centrifugal force and their rotation frequency is affected by this effective gravitational force, while the electrons are driven by

both the $\mathbf{E} \times \mathbf{B}$ drift and the diamagnetic drift. The difference between the azimuthal drift velocities of the ions and electrons induce charge separation which cannot be fully neutralized by the electrons whose axial motions are dragged by the collisions with neutral particles. Thus fluctuations are excited and azimuthal motions are organized in such a way that the core part of the plasmas is rotating almost rigidly, while the outer part lags behind the core part because the azimuthal drift velocities do not increase in proportion to the radius, consequently producing a spiral structure.

Equations for ions and electrons in magnetized plasmas read

$$\frac{\partial n_\alpha}{\partial t} + \nabla(n_\alpha \mathbf{v}_\alpha) = 0, \tag{1}$$

$$\frac{\partial \mathbf{v}_\alpha}{\partial t} + \mathbf{v}_\alpha \cdot \nabla \mathbf{v}_\alpha = \frac{e_\alpha}{m_\alpha}(-\nabla\phi + \frac{1}{c}\mathbf{v}_\alpha \times \mathbf{B}) - \delta_{\alpha,e}\frac{1}{nm_\alpha}\nabla p_\alpha - \nu_\alpha \mathbf{v}_\alpha. \tag{2}$$

where n_α, $\mathbf{v}_\alpha$ and ν_α ($\alpha = e$ or i) are the density, velocity and collision frequency with neutral particles of electrons and ions, respectively, and ϕ is the plasma potential. Usually the ion temperature is much less than the electron temperature in laboratory plasmas, we neglect the ion pressure term in Eq.(2), for simplicity ($\delta_{\alpha,e} = 1$ for $\alpha = e$, and 0 for $\alpha = i$).

In the following, physical quantities are divided into the stationary parts and fluctuating parts:

$$\begin{pmatrix} n \\ \phi \\ \mathbf{v} \end{pmatrix} = \begin{pmatrix} n_0(r,z) \\ \phi_0(r,z) \\ \mathbf{v}_0(r,z) \end{pmatrix} + \sum_\ell \begin{pmatrix} n_\ell(r,z) \\ \phi_\ell(r,z) \\ \mathbf{v}_\ell(r,z) \end{pmatrix} e^{i(\ell\theta - \omega t)} + c.c.$$

For the ion drift, an effective gravitational drift due to the centrifugal force is taken into account in the azimuthal direction, and is neglected in the radial direction since $\nu_i/\Omega_i << 1$. For the electron drift, the diamagnetic drift is dominated over the gravitational drift due to the centrifugal force. The rotation frequencies of the ion and electron azimuthal drift now read

$$\omega_0^i \simeq \omega_E(1 - \frac{\omega_E}{\Omega_i}), \quad \omega_0^e \simeq \omega_E + \omega_*, \tag{3}$$

where ω_E and ω_* are the frequencies associated with the $\mathbf{E} \times \mathbf{B}$ drift and the diamagnetic drift, respectively, defined by

$$\omega_E = \frac{C_s^2}{\Omega_i}\frac{1}{r}\frac{d\phi_0}{dr}, \quad \omega_* = -\frac{v_T^2}{\Omega_e}\frac{1}{r}\frac{d\ln n_0}{dr}, \tag{4}$$

where $C_s^2 = T_e/M$, $v_T^2 = T_e/m$, $\Omega_i = eB/Mc$ and $\Omega_e = eB/mc$ (M: ion mass, m: electron mass). The normalized potential $e\phi_0/T_e$ has been replaced by ϕ_0 in Eq.(4). The second term in the expression for ω_0^i is a contribution from the centrifugal force.

The space potential produced by the ion radial transport is short-circuited by the electron axial transport so that we have $\nabla(n_0^i \mathbf{v}_0^i) = \nabla(n_0^e \mathbf{v}_0^e)$, which determines the profile of the equilibrium density and potential. Since the solution of this equation is sensitively dependent on the boundary conditions at the end of the field lines unless the plasma is so long that parallel diffusion can be neglected altogether, it is unlikely to obtain a self-consistent solution $n_0(r,z)$ and $\phi_0(r,z)$ to the problem of ambipolar diffusion across the magnetic field. Instead, in the following we take a phenomenological approach to assume the density and potential profiles compatible with those observed in the experiment.

The fluctuating parts of electron velocities given by Eqs.(1) and (2) are

$$\begin{aligned}
u_\ell^e &= \frac{v_T^2}{\Sigma_e(\omega)}[-\frac{i\ell(\Omega_e - 2\omega_0^e)}{r} + \Gamma_e(\omega)\frac{\partial}{\partial r}](\phi_\ell - \frac{n_\ell^e}{n_0}), \\
v_\ell^e &= \frac{v_T^2}{\Sigma_e(\omega)}[(\Omega_e - \omega_0^e - \frac{dv_0^e}{dr})\frac{\partial}{\partial r} + \frac{i\ell\Gamma_e(\omega)}{r}](\phi_\ell - \frac{n_\ell^e}{n_0}), \\
w_\ell^e &= \frac{v_T^2}{\Gamma_e(\omega)}\frac{\partial}{\partial z}(\phi_\ell - \frac{n_\ell^e}{n_0}),
\end{aligned}$$

where $u_\ell^e, v_\ell^e, w_\ell^e$ are the radial, azimuthal and axial component of $\mathbf{v}_\ell^e$, respectively, and

$$\begin{aligned}
\Gamma_e(\omega) &= \nu_e - i(\omega - \ell\omega_0^e), \\
\Sigma_e(\omega) &= (\Omega_e - 2\omega_0^e)(\Omega_e - \omega_0^e - \frac{dv_0^e}{dr}) + \Gamma_e(\omega)^2.
\end{aligned}$$

where v_0^e is the zeroth order azimuthal drift velocity for electrons ($v_0^e = r\omega_0^e$). The fluctuating parts of ion velocities $u_\ell^i, v_\ell^i, w_\ell^i$ are also obtained in a similar calculations.

Substituting the above velocities into the electron and ion continuity equations, invoking charge neutrality $n_\ell^e = n_\ell^i = n_\ell$, and assuming the axial dependence of the potential with the normalizations $\xi = r/r_d$ and $\eta = z/r_d$ (r_d: plasma radius) as

$$\phi_\ell(\xi, \eta) = \phi_\ell(\xi) e^{-(\kappa - ik)\eta}, \tag{5}$$

we have

$$\frac{d^2\phi_\ell}{d\xi^2} + [\frac{1}{\xi} + \frac{d \ln n_0}{d\xi}]\frac{d\phi_\ell}{d\xi} + [\beta(\xi) - \frac{\ell^2}{\xi^2}]\phi_\ell = 0, \tag{6}$$

where the quantity $\beta(\xi)$ is given by

$$\beta(\xi) = \frac{(\kappa - ik)^2 \Omega_e \Omega_i}{\Gamma_e(\omega)\Gamma_i(\omega)}(1 - \frac{\ell\omega_*}{\omega - \ell\omega_E}) - \frac{i\ell}{\xi}\frac{1}{\Gamma_i(\omega)}\Big[(\omega_0^i + \frac{1}{r_d}\frac{dv_0^i}{d\xi} + \frac{\ell\omega_E^2}{\omega - \ell\omega_E})\frac{d \ln n_0}{d\xi} + \frac{d\omega_0^i}{d\xi} + \frac{1}{r_d}\frac{d^2 v_0^i}{d\xi^2}\Big]. \tag{7}$$

In deriving Eq.(6), we have neglected the terms of the order of or less than $O(\Omega_i/\Omega_e)$ and $O(\omega_0^i/\Omega_i)$, and used the following approximation derived from the electron or ion continuity equation,

$$\frac{n_\ell}{n_0} \simeq -\frac{v_T^2}{\Omega_e^2}\frac{\ell\Omega_e}{\omega - \ell(\omega_0^e - \omega_*)}\frac{1}{r}\frac{d \ln n_0}{dr}\phi_\ell = \frac{\ell\omega_*}{\omega - \ell\omega_E}\phi_\ell. \tag{8}$$

Equation (6) describes low frequency fluctuations excited by collisional drift wave instability (the first term of $\beta(\xi)$) [9] and flute mode instability such as the gravitational instability due to centrifugal force acting on ions (the second term of $\beta(\xi)$) [10] and Kelvin-Helmholz instability (the third and fourth terms of $\beta(\xi)$) [11]. The difference between Eq.(6) and the equation derived by Rosenbulth and Simon [8] is that the collisional drag is taken into account and the charge neutrality is assumed in Eq.(6), while in Ref. [8] the collisional drag is not included and the ion diamagnetic drift is taken into account instead of the electron diamagnetic drift. Putting that $\phi_\ell(\xi) = \psi_\ell(\xi)/\sqrt{n_0(\xi)}$, Eq.(6) is transformed to

$$\frac{d^2\psi_\ell}{d\xi^2} + \frac{1}{\xi}\frac{d\psi_\ell}{d\xi} + [A(\xi) - \frac{\ell^2}{\xi^2}]\psi_\ell = 0. \tag{9}$$

The ratio of the contribution from the drift wave to that from the flute mode is estimated to be $(\kappa^2 + k^2)(\Omega_e/\nu_e)(r_d\Omega_i/C_s)$. The collisional drift wave instability is dominant when

$\kappa^2 + k^2 >> (\nu_e/\Omega_e)(C_s/r_d\Omega_i)$ is satisfied. The quantity $(\nu_e/\Omega_e)(C_s/r_d\Omega_i)$ is of the order of 10^{-4} to 10^{-5} for the ECR plasmas and thus we only consider the fluctuations due to the collisional drift wave instability:

$$A(\xi) \simeq \frac{(\kappa - ik)^2\Omega_e\Omega_i}{\Gamma_e(\omega)\Gamma_i(\omega)} \frac{(\omega - \ell\omega_0^e)}{(\omega - \ell\omega_E)}.$$

Now the characteristic features of the solutions for Eq.(9) can be examined as follows. The solution is approximated in the case of weak ξ-dependence of the zeroth order quantities by $\psi_\ell(\xi) \simeq J_\ell(\xi\sqrt{A})$, where J_ℓ is the Bessel function of the first kind. The real part of the argument of the Bessel function should be positive to give a convergent behavior while the imaginary part is responsible for spiral structure, which comes from the imaginary parts of ω, $\Gamma_e(\omega)$ and $\Gamma_i(\omega)$. Multiplying ψ_ℓ^* to Eq.(9) and integrating the resultant equation from the center to the edge of the plasma under the boundary condition $\psi_\ell(0) = \psi_\ell(1) = 0$, we have

$$\int_0^1 \xi\{|\frac{d\psi_\ell}{d\xi}|^2 + \frac{\ell^2}{\xi^2}|\psi_\ell|^2 - A(\xi)|\psi_\ell|^2\}d\xi = 0. \tag{10}$$

From the imaginary part of this equation we have

$$\int \Im[A(\xi)]\xi|\psi_\ell(\xi)|^2 d\xi = 0, \tag{11}$$

which corresponds to the Rayleigh condition. For a collisional drift mode, we have at the marginal instability ($\gamma \sim 0$) with $\kappa >> k$

$$\Im[A(\xi)] = \frac{\nu_e\kappa^2\Omega_e\Omega_i(\omega_r - \ell\omega_0^e)(\omega_r - \ell\omega_0^i)(\omega_r - \ell\omega_E)}{|\Gamma_e(\omega)|^2|\Gamma_i(\omega)|^2[(\omega_r - \ell\omega_E)^2 + \gamma^2]},$$

from which the Rayleigh condition holds even when $\omega_r = 0$, indicating the formation of stationary spiral structures. The winding direction of spiral arms is reversed when the magnetic fields is changed in sign since the imaginary part of $A(\xi)$ is proportional to odd power of the magnetic field for $\omega_r = 0$. Certainly rotating spirals exist as well.

Here we solve Eq.(6) numerically with the boundary condition $\phi_\ell(0) = \phi_\ell(1) = 0$. Since, according to the experimental observations, the profile of $\mathbf{E} \times \mathbf{B}$ drift frequency ω_E has

one zero between $\xi = 0$ and $\xi = 1$, we have used the ω_E profile as shown in Fig.1 in the calculations. Furthermore, the density profile $n_0(r)$ has been assumed to be Gaussian, from which the diamagnetic drift frequency ω_* is depicted in the same figure. We have both the stationary ($\omega_r = 0$) and rotating ($\omega_r \neq 0$) spiral solutions for a given profile of the zeroth order quantities $n_0(r)$ and $\omega_E(r)$. The numerical results for the stationary solution ($\ell = 2$) are shown in Fig.2, where Fig.2(a) is the radial potential profile, and Fig.2(b) the density perturbation contour calculated by Eq.(8). The spiral structure is identified as an Archimedes spiral, which is seen from the eikonal approximation for the solution of Eq.(6); in the case of weak $\xi-$dependence of $\beta(\xi)$, $\phi_\ell(\xi)\exp[i\ell\theta] \sim \exp[i\int \Re[\sqrt{\beta}]d\xi + i\ell\theta] \sim \exp[i\Re[\sqrt{\beta}]\xi + i\ell\theta]$ and the spiral curves are given by $\xi \propto \theta$. The density contour structure is similar to the observed spiral.

The vector field plot of the ion velocity $\{u^i_\ell, v^i_\ell\}$ associated with this spiral structure is depicted in Fig.3. In the figure, each arrow is colored by red for positive radial velocity $u^i_\ell > 0$ and by green for negative radial velocity $u^i_\ell < 0$. The flow pattern exhibits the similar spiral structure, which well explained by the $\mathbf{E} \times \mathbf{B}$ drift due to the perturbed potential ϕ_ℓ. It should be noted that the spiral structure induces both the outward-going (counterclockwise) flow and the inward-going (clockwise) flow, exhibiting a material circulation between the core and peripheral regions.

The imaginary part of the eigenvalue γ decreases with the azimuthal mode number ℓ, which corresponds to the fact that the observed stationary spirals are always with two arms.

The mass ratio of ion and electron is taken to be 80000 in the above calculations since the experiments were curried out in an argon plasma. The spiral solutions are independent on the mass ratio and also obtained for the hydrogen case ($M/m = 2000$).

Even when we neglect the contributions from the centrifugal and the Kelvin-Helmholz instabilities in Eq.(6), there is no change in the pattern of the spiral. Thus, the spiral structure formation for this choice of parameters is attributable to the collisional drift wave instability.

In the numerical calculations, we have used the special profile for the $n_0(r)$ and $\omega_E(r)$

since we need to compare the numerically obtained spirals with those observed in the experiment [4]. However, it has been confirmed that the spiral solutions of Eq.(6) are insensitive to the profiles of these quantities.

For the different parameters ($\Re[\omega] = 0$, $\Im[\omega] = 0.27$, $\kappa = 0.115$, k = 0.0259), a granulated density structure is obtained, which is regarded as a formation of vortex crystal. Although the vortex crystallization has been reported in pure electron plasmas [2], this type of structures may be general entities excited in magnetized plasmas.

It should be noted that we used the $e^{-(\kappa - ik)\eta}$ as an axial mode function to include the axial variations observed in the experiment. When we set $\kappa = 0$, we have also obtained spiral solutions as shown in Fig.2. Thus, the finiteness of κ does not affect the spiral pattern formation. Strictly, the axial profile is determined in the higher order equations in terms of smallness parameter associated with the fluctuation quantities. Nonlinear calculations show that the axial profile is generated by the balance between dispersion, diffusion and nonlinearlity, and is written by the Gintzburg-Landau equation, which admits localized solutions [12]. Since the mechanism of axial structure formation is different from that of radial pattern in the present case, the nonlinear results are omitted here, and will be reported elsewhere.

Formation of spiral structures is a rather general characteristic of magnetized rotating plasmas since the energy stored in the plasma inhomogeneity such as density and velocity shear is released to give instabilities, which cause the phase difference between the real and imaginary parts of eigen-functions, driving a spiral structure. The instabilities could be the collisional drift wave instability, centrifugal instability, Kelvin-Helmholz instability, and inhomogeneous energy-density driven instability (IEED) [6,13]. In the present case, in which $(\kappa^2 + k^2) \gg (\Omega_e/\nu_e)(r_d\Omega_i/C_s)$ is satisfied, the drift wave instability is dominant, which is destabilized by collisions. Thus, the collision play a key role on the formation of drift wave spiral.

Under the special condition that $\omega_E(\xi)$ becomes zero somewhere between $\xi = 0$ and $\xi = 1$, the characteristic of the stationary spiral structure becomes similar to those observed in the

experiment. For a wide variety of density and potential profiles, rotating spiral structures are normally excited.

We have obtained the linear eigen-functions to show the spiral structure formations in magnetized rotating plasmas. We are planning to develop our theory to understand the spiral structures observed in a gun-produced plasma [5]. It is worth noting that our study may contribute for understanding the mechanism of spiral galaxy formation.

REFERENCES

[1] M.V. Nezlin and E.N. Snezhkin, *Rossby Vortices, Spiral Structures, Solitons*, (Springer-Verlag, Berlin, 1993).

[2] K.S. Fine, A.C. Case, W.G. Flynn and C.F. Driscoll, Phys. Rev. Lett. **75**, 3277 (1995).

[3] Y. Amagishi, Y. Yoshikawa and J. Ohara, J. Phys. Soc. Jpn **60**, 2496 (1992).

[4] M.Y. Tanaka, T. Sakamoto, H. Imaizumi, K. Taniguchi and Y. Kawai, Proc. 1996 Int. Conf. on Plasma Physics (Nagoya, Japan) Vol.2, 1650 (1997).

[5] T. Ikehata, H. Tanaka, N.Y. Sato and H. Mase, Phys. Rev. Lett. **81**, 1853 (1998).

[6] W.E. Amatucci et al., Phys. Rev. Lett. **77**, 1978 (1996).

[7] J.R. Peñano, G. Ganguli, W.E. Amatucci, D.N. Walker, V. Gavrishchaka, Phys. Plasmas **5**, 4377 (1998).

[8] M.N. Rosenbulth and A. Simon, Phys. Fluids **8** 1300 (1965).

[9] F.F. Chen, Phys. Fluids **10**, 1647 (1967).

[10] A.B. Mikhailovskii, *Theory of Plasma Instabilities, vol.2* Chap.7, (Consultants Bureau, New York, 1974).

[11] C.C. Lin, *The Theory of Hydrodynamic Stability*, (Cambridge University Press, Cambridge, 1966).

[12] K. Nozaki and N. Bekki, J. Phys. Soc. Jpn **53** 1581 (1984).

[13] M.E. Koepke, W.E. Amatucci, J.J. Carroll III, and T.E. Sheridan, Phys. Rev. Lett. **72**, 3355 (1996).

FIGURES

FIG. 1. The radial profiles of the normalized $\mathbf{E} \times \mathbf{B}$ drift frequency ω_E/Ω_i and the normalized diamagnetic drift frequency ω_*/Ω_i.

FIG. 2. The numerical results for a stationary spiral solution ($M/m = 80000$, $\kappa = 0.0675$, $k = 0.0225$, $\gamma/\Omega = 0.024$). (a): the radial profile of the perturbed potential $\phi_\ell(\xi)$, in which the solid line is the real part, and the dotted line the imaginary part. (b): the density perturbation contour $\Re[(n_\ell/n_0)\exp(i\ell\theta)]$.

FIG. 3. The vector field plot of ion velocity associated with the spiral structure corresponding to Fig.2 ($u^i_\ell > 0$: red; $u^i_\ell < 0$: green).

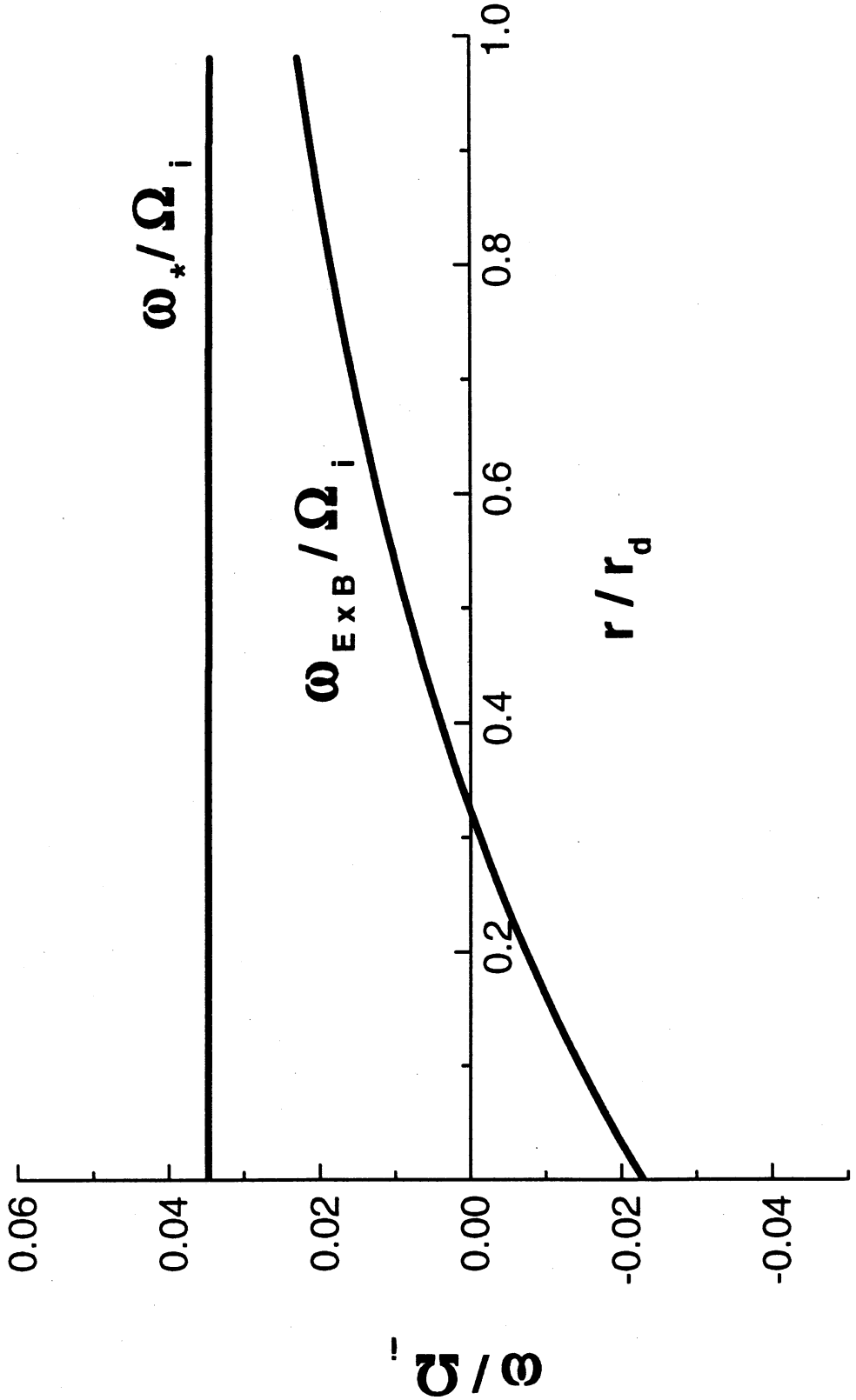

Fig. 1

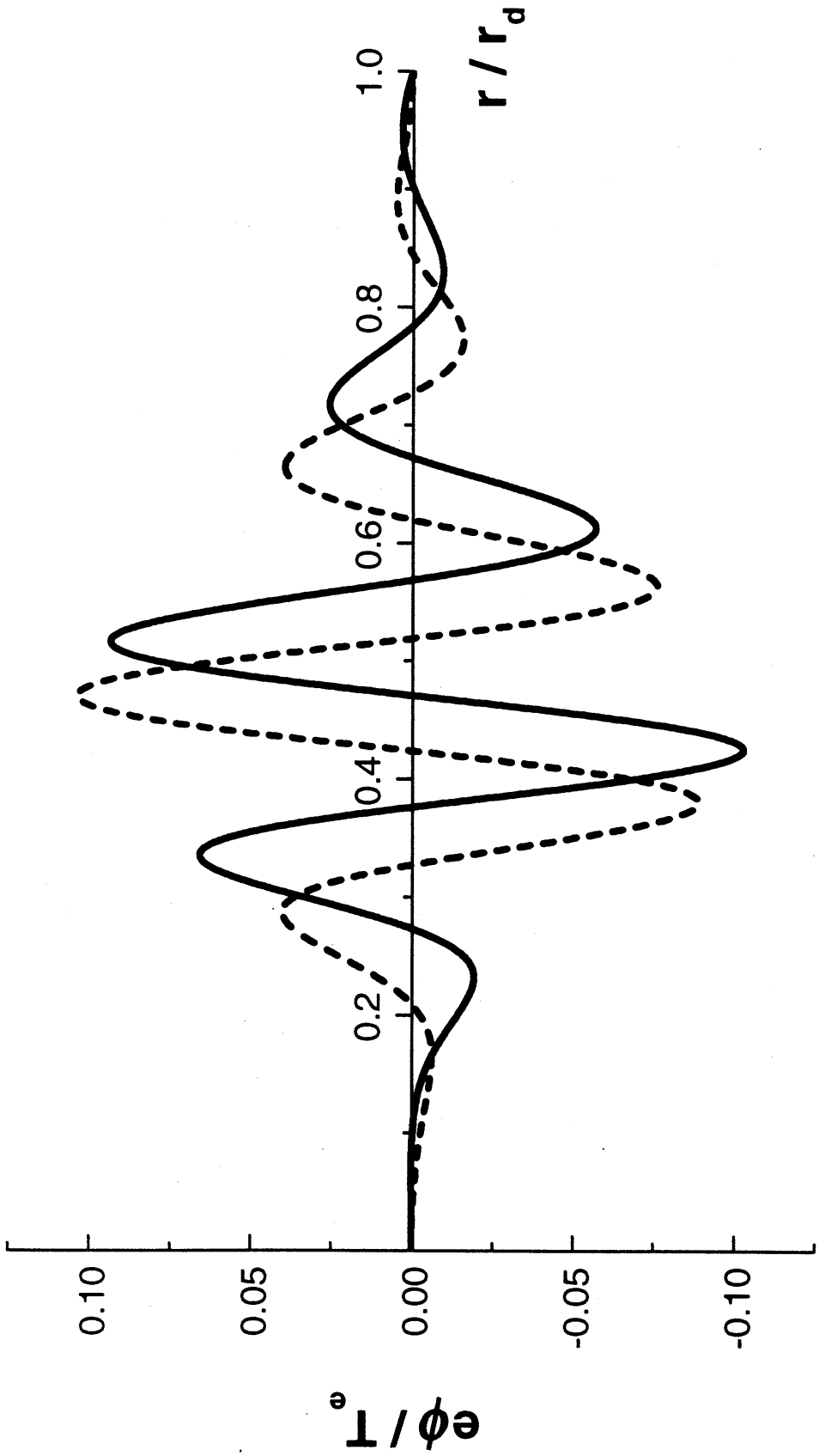

Fig. 2(a)

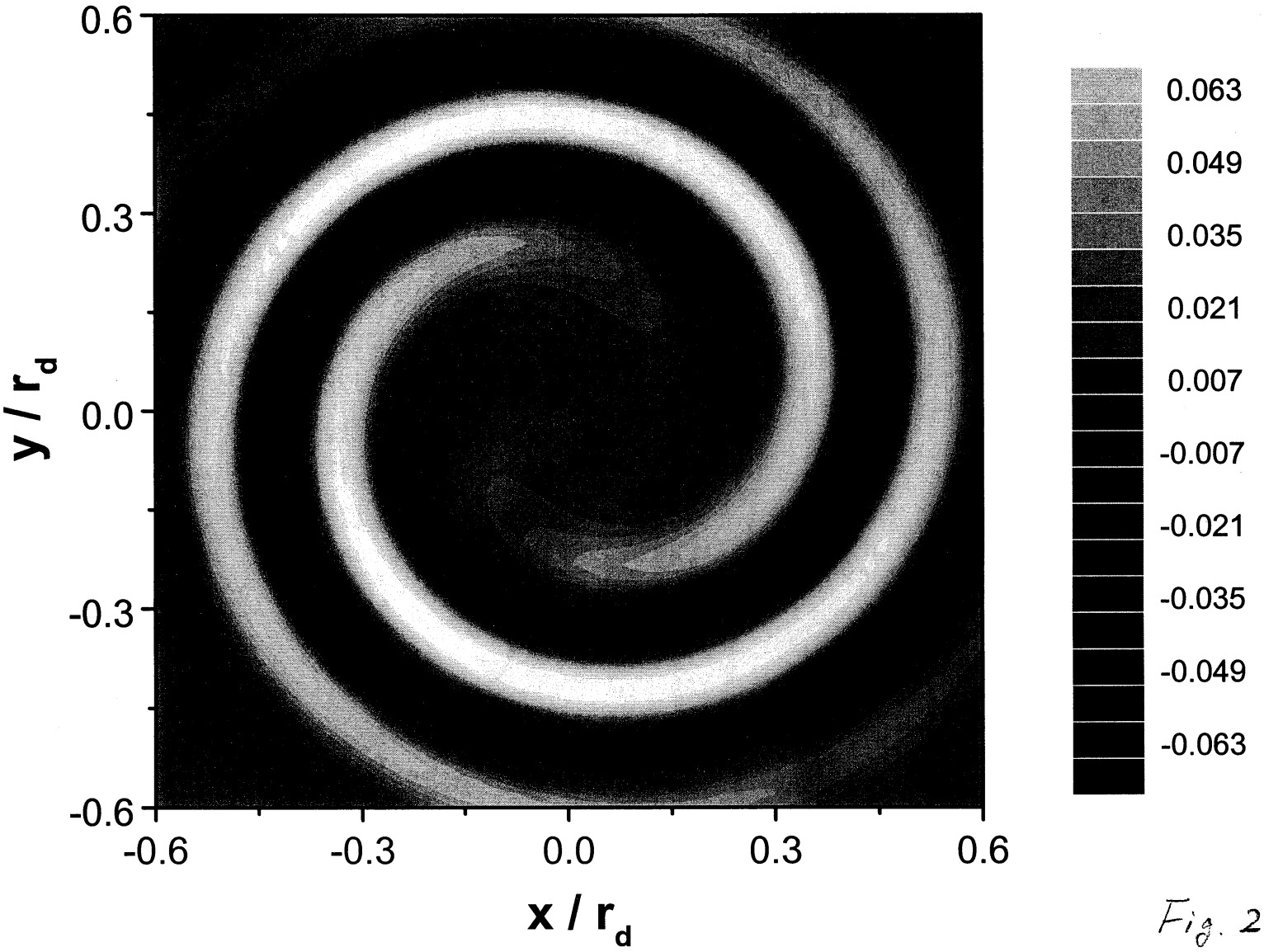
0.6
0.3
0.0
-0.3
-0.6
y / r_d
-0.6
-0.3
0.0
0.3
0.6
x / r_d
0.063
0.049
0.035
0.021
0.007
-0.007
-0.021
-0.035
-0.049
-0.063

Fig. 2(b)

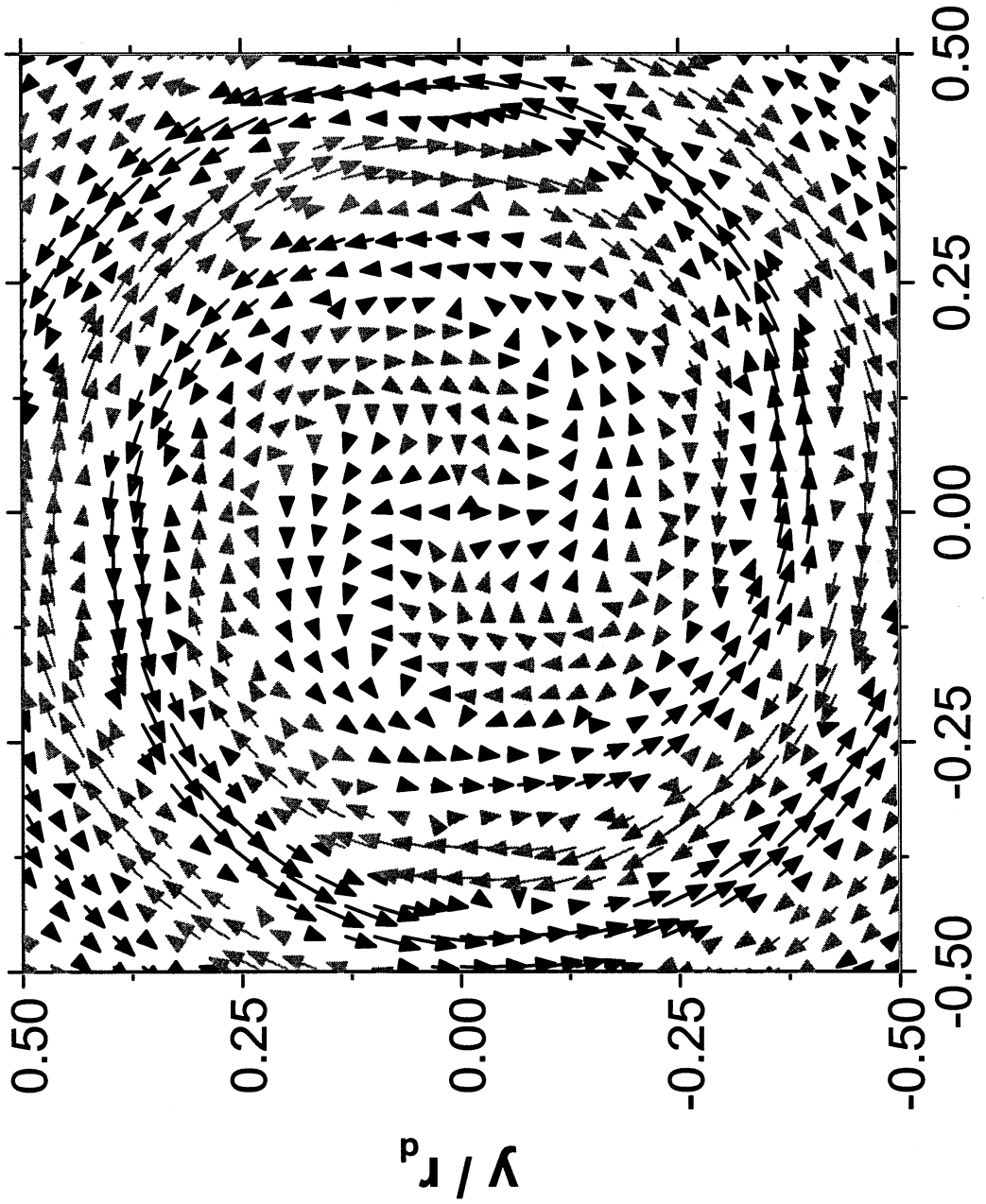

Fig. 3